

DTIC FILE COPY

Naval Research Laboratory

Washington, DC 20375-5000

NRL Publication 167-6320

May 1990



AD-A222 432

IC 1990 D

6

Annual Report

October 1988 — November 1989

Office of Naval Research

Contract Number N0001490WX24009

**Passivity Mechanisms of Surfaces Produced  
by Ion Beam Mixing and Ion Implantation**

P. M. NATISHAN, E. MCCAFFERTY,  
AND G. K. HUBLER

*Physical Metallurgy Branch  
Materials Science and Technology Division  
Naval Research Laboratory  
Washington, DC 20375*

Approved for public release, distribution unlimited.

06 06 05 085

UNCLASSIFIED

SECURITY CLASSIFICATION OF THIS PAGE

## REPORT DOCUMENTATION PAGE

1a. REPORT SECURITY CLASSIFICATION UNCLASSIFIED		1b. RESTRICTIVE MARKINGS NONE	
2a. SECURITY CLASSIFICATION AUTHORITY		3. DISTRIBUTION/AVAILABILITY OF REPORT  UNLIMITED	
2b. DECLASSIFICATION/DOWNGRADING SCHEDULE NONE			
4. PERFORMING ORGANIZATION REPORT NUMBER(S)		5. MONITORING ORGANIZATION REPORT NUMBER(S) NRL Publication 167-6320	
6a. NAME OF PERFORMING ORGANIZATION  Naval Research Laboratory	6b. OFFICE SYMBOL (If applicable)	7a. NAME OF MONITORING ORGANIZATION	
6c. ADDRESS (City, State, and ZIP Code) Code 6322 Naval Research Laboratory Washington, DC 20375-5000		7b. ADDRESS (City, State, and ZIP Code)	
8a. NAME OF FUNDING/SPONSORING ORGANIZATION  Office of Naval Research	8b. OFFICE SYMBOL (If applicable)	9. PROCUREMENT INSTRUMENT IDENTIFICATION NUMBER N0001490WX24009	
8c. ADDRESS (City, State, and ZIP Code) 800 N. Quincy Street ARLINGTON, VA 22217-5000		10. SOURCE OF FUNDING NUMBERS	
		PROGRAM ELEMENT NO	PROJECT NO
		TASK NO	WORK UNIT ACCESSION NO.
11. TITLE (Include Security Classification) (U) Passivity of Mechanisms of Surfaces Produced by Ion Beam Mixing and Ion Implantation			
12. PERSONAL AUTHOR(S) P.M. Natishan, E. McCafferty, G.K. Hubler			
13a. TYPE OF REPORT Annual	13b. TIME COVERED FROM 10/1/89 TO 11/30/89	14. DATE OF REPORT (Year, Month, Day) May 1990	15. PAGE COUNT 26
16. SUPPLEMENTARY NOTATION			
17. COSATI CODES	18. SUBJECT TERMS (Continue on reverse if necessary and identify by block number)  (Sub p2c)		
FIELD			
19. ABSTRACT (Continue on reverse if necessary and identify by block number)			
<p>The corrosion behavior of Mo-Al, Cr-Al and Cr-Mo-Al surface alloys produced by ion implantation and ion beam mixing was examined in deaerated, 0.1M NaCl. The polarization behavior of the ion implanted samples was similar to that of Al and the pitting potentials of the ion implanted samples were 115 to 155 mV higher than that of Al. From the standpoint of the <sup>ppc</sup> model this behavior would be explained by the presence of the implanted cations in the stable oxide lattice. There was incomplete mixing of the coating and substrate for the ion beam mixed samples, and the mixed elements remained almost entirely in the metallic state so that the desired mixed oxide films were not formed. Ion beam mixing did impart additional stability compared to as-deposited samples since the mixing process produced more compact coatings.</p> <p style="text-align: right;">(KR)</p>			
20. DISTRIBUTION/AVAILABILITY OF ABSTRACT <input checked="" type="checkbox"/> UNCLASSIFIED/UNLIMITED <input type="checkbox"/> SAME AS RPT <input type="checkbox"/> DTIC USERS		21. ABSTRACT SECURITY CLASSIFICATION UNCLASSIFIED	
22a. NAME OF RESPONSIBLE INDIVIDUAL E. McCAFFERTY and P.M. NATISHAN		22b. TELEPHONE (Include Area Code) (202) 767-1344	22c. OFFICE SYMBOL Code 6322

## Table of Contents

I. Introduction.....	1
II. Experimental Methods.....	4
III. Results and Discussion.....	6
A. Untreated Metals.....	6
B. Ion Implantation.....	6
C. Ion Beam Mixing.....	11
IV. Summary.....	22
V. Acknowledgments.....	23
VI. References.....	24

Accession For	
Printed	PPA&I
110-710	<input checked="" type="checkbox"/>
for Periodicals	<input type="checkbox"/>
for Collection	<input type="checkbox"/>
Date Received	
1/1/68	
Date Entered	
1/1/68	
Serials	
A-1	



A-1

## I. INTRODUCTION

The mechanism of anion adsorption, the first step in passive film breakdown leading to localized corrosion, has been described by a model based on surface charge considerations and the pH of zero charge of an oxide,  $\text{pH}_{\text{pzc}}$  (1,2). At the  $\text{pH}_{\text{pzc}}$  the surface of an oxide has no net charge. At pHs lower than the  $\text{pH}_{\text{pzc}}$ , the surface has a net positive charge, and anions such as chloride are electrostatically attracted to the surface and can become incorporated into the oxide film. The incorporated anions cause film disruption and loss of passivity. At pHs higher than the  $\text{pH}_{\text{pzc}}$ , the surface has a net negative charge and anion adsorption is inhibited.

The  $\text{pH}_{\text{pzc}}$  model predicts that the surface charge of an oxide such as aluminum oxide can be changed by introducing other oxide-forming elements into the oxide film and thereby increasing or decreasing anion adsorption and the susceptibility to localized corrosion. Experimental results for binary aluminum surface alloys produced by ion implantation lend support to this model. As shown in Figure 1, ion implantation with elements such as Mo, Si, Cr, Zr and Nb for which the oxides have a  $\text{pH}_{\text{pzc}}$  lower than that of aluminum oxide increased the pitting resistance of aluminum, whereas implantation with Zn, for which the oxide has a higher  $\text{pH}_{\text{pzc}}$  than aluminum oxide, decreased the pitting resistance of aluminum (1,2).

One factor that prevented a more quantitative correlation between the pitting potential and the  $\text{pH}_{\text{pzc}}$  was that the surface concentration of the implanted species was lower than desired and varied with the implanted species. For example, the actual surface concentrations of the implanted elements for the Si-Al, Zr-Al and Mo-Al surface alloys, shown in Figure 1

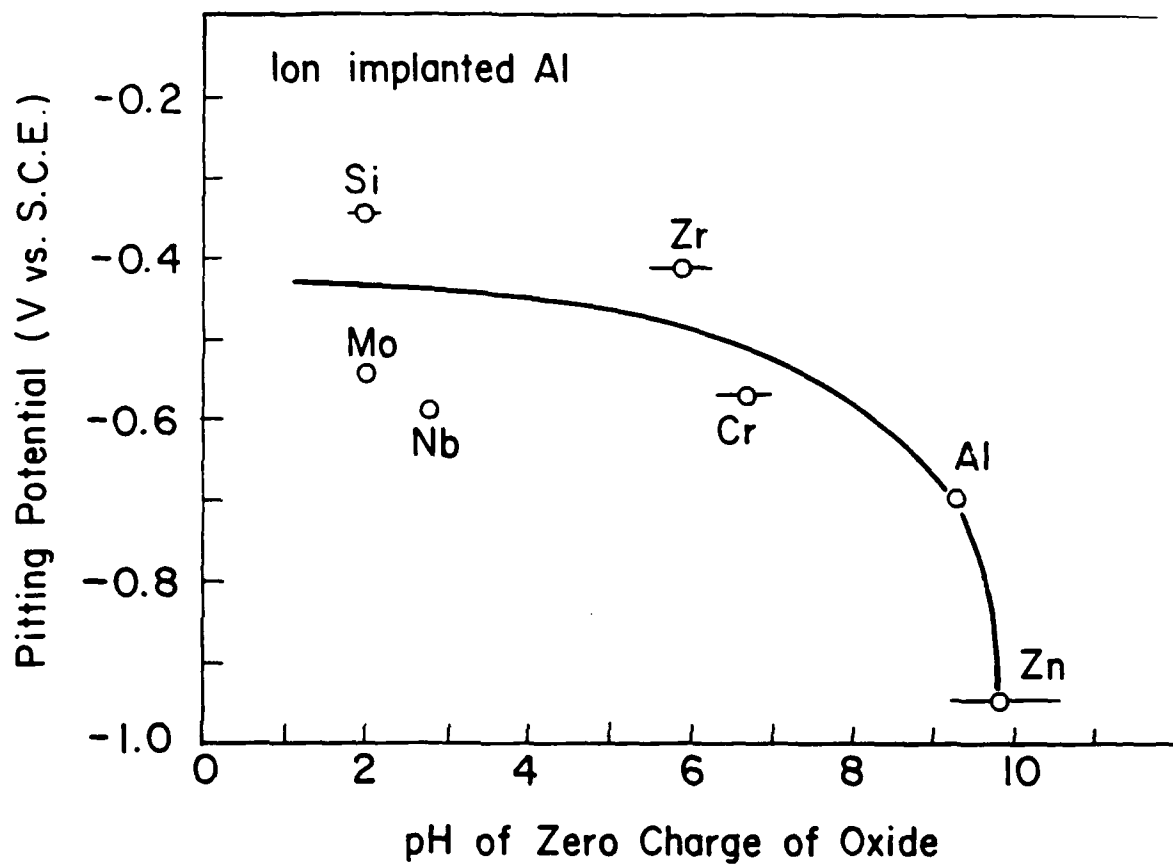


Figure 1. Pitting potentials of the nominal 12 a/o ion implanted samples in 0.1M NaCl vs. the pH of zero charge of the oxide of the implanted species.

were 8, 4 and approximately 2 atomic percent (a/o), respectively. Also, in some some cases the surface concentration of the implanted species was independent of the implantation dose. When Mo was ion implanted under conditions that were to yield nominal surface concentrations of 4, 12, or 20 a/o, the actual surface concentration for all alloys was approximately 1 to 2 a/o (1,2). These effects were caused by radiation enhanced diffusion, radiation induced segregation, and/or ion channelling. (1,2)

In order to further study the relationship between the pitting potentials and the pH<sub>pzc</sub> and to produce surface alloys of engineering significance, it is necessary to produce surface alloys with higher, more consistent surface concentrations of the alloying element. Ion beam mixing is an extension of ion implantation in which a sputter deposited or evaporated thin film of several hundreds to thousands angstroms thickness is induced to intermix with the substrate using the collisional cascades generated by bombardment with an inert ion, such as xenon or argon, or with an ion that can be chemically reactive, such as chromium or molybdenum. Ion beam mixing retains all of the advantages of ion implantation and offers a method of producing surface alloys with higher surface concentrations of the alloying element. In addition, previous work indicates that ion beam mixing is a promising technique for producing samples with improved corrosion resistance (2,3). This communication reports on the anodic behavior of Mo-Al, Cr-Al and Cr-Mo-Al surface alloys produced by ion implantation and by ion beam mixing.

## II. EXPERIMENTAL METHOD

Because ion beam modification is a line of sight process, it was important to prepare flat, featureless surfaces. Samples were cut from a 3/4 inch diameter aluminum rod (99.999% pure) and were polished automatically. The final polish was performed on a polishing wheel using 0.06  $\mu\text{m}$   $\text{SiO}_2$  in a basic suspension so that the final step was a chemical as well as a mechanical polish. Final polishing times did not exceed 3 minutes. Chromium and molybdenum samples were polished to a 3  $\mu\text{m}$  finish using diamond spray.

After polishing, the aluminum samples were implanted with a selected ion (Mo, Cr, or Cr+Mo) using the conditions described in Table 1. The samples were clamped to a water-cooled heat sink to maintain temperatures less than 30°C during ion implantation and the vacuum was 0.8 to  $2 \times 10^{-6}$  torr. The samples were implanted to produce a depth concentration profile that had a peak concentration nominally at the surface extending 500 angstroms into the bulk before decreasing. Samples were analyzed before and after pitting by Rutherford backscattering spectroscopy (RBS) and in some instances by X-ray photoelectron spectroscopy (XPS). RBS data on as-polished and as-implanted samples indicated surface oxygen concentrations of 15 to  $30 \times 10^{15}$  atoms/cm<sup>2</sup> computed as 21 to 42 Å of stoichiometric  $\text{Al}_2\text{O}_3$ . RBS profiles were obtained with a 2 MeV alpha-particle beam produced by the NRL 5 MV Van de Graaff accelerator. A glancing angle of detection of 8° from the surface plane was used to enhance the depth resolution; the scattering angle was 135°.

X-ray photoelectron spectroscopy (XPS) measurements were made using a Surface Science Laboratories, Inc. Model SSX-100-03 spectrophotometer with a monochromatic Al  $K\alpha$  X-ray source. The spot size was either 600 or 300  $\mu\text{m}$ ; and the pass energy was 100 eV. The base pressure was  $8 \times 10^{-9}$  torr or better. The XPS spectra were corrected for charge shifts by normalizing binding energies to that of the carbon 1s peak of adventitious carbon at 284.6 eV (4).

Mo-Al, Cr-Al and Cr-Mo-Al ion beam mixed surface alloys were prepared as follows. A 100 to 300  $\text{\AA}$  coating of the selected element(s) was vapor or sputter deposited onto an aluminum substrate, and mixing was then accomplished with  $\text{Xe}^+$ ,  $\text{Xe}^{++}$ ,  $\text{Cr}^+$  or  $\text{Mo}^+$  ions at energies from 110 to 250 keV. A complete listing of preparative conditions is given in Table 2. The ion beam mixed samples were examined with RBS and XPS before and after pitting corrosion experiments.

Samples were attached to electrode holders, and the sample sides and the edge of the face to be tested were masked with several coats of an alkyd varnish. The electrochemical measurements were made in a deaerated 0.1M NaCl solution using a conventional corrosion cell. The 0.1M NaCl solution was made with reagent grade NaCl and triply distilled water prepared in a quartz still. The solution pH was approximately 6; argon was used to deaerate the solution. The samples were immersed in the solution for 24 hours to establish a steady state open circuit potential. The pitting potentials for ion implanted, ion beam mixed, and untreated metal (Al, Cr, and Mo) samples were then determined potentiostatically by stepping the potential in 25 to 50 mV increments from the corrosion potential in the anodic direction allowing the current to reach steady state values. Usually 16 to 20 minutes were required at each potential.

### III. Results and Discussion

#### A. Untreated Metals

Anodic polarization curves for Al, Mo, and Cr are shown in Figure 2. The polarization curve for Al show that Al has a large passive range and that pitting occurs at -0.700 V<sub>sce</sub>. The polarization curves for Mo and Cr, and subsequent optical examination show that both metals undergo general dissolution. This behavior has been observed previously for Mo in a variety of electrolytes (5,6). It has been shown that Cr exhibits active-passive behavior in 1M H<sub>2</sub>SO<sub>4</sub> and HCl ( 6,7 ), but in this investigation, both Mo and Cr were unable to form passive films in deaerated 0.1M NaCl.

#### B. Ion Implantation

As has been discussed above and elsewhere (1,2), the desired depth concentration profiles for the implanted species were not obtained due to radiation enhanced diffusion, radiation induced segregation and/or ion channelling. (1,2) For example, the XPS depth concentration profile presented in Figure 3 shows that the actual surface concentration of Cr in the surface alloy that was implanted at doses to produce a 12 a/o Cr surface alloy was actually about 1 to 2 a/o. Figure 4 shows the anodic polarization curves for Al and the Cr-Al surface alloy. It can be seen that the effect of implantation with Cr was to increase the pitting potential of Al by 135 mV. It has been demonstrated previously that the physical damage due to ion implantation does not affect the pitting potential and that improvements in the pitting potential from various implanted species can be attributed to chemical effects (1). Table 1 summarizes the results

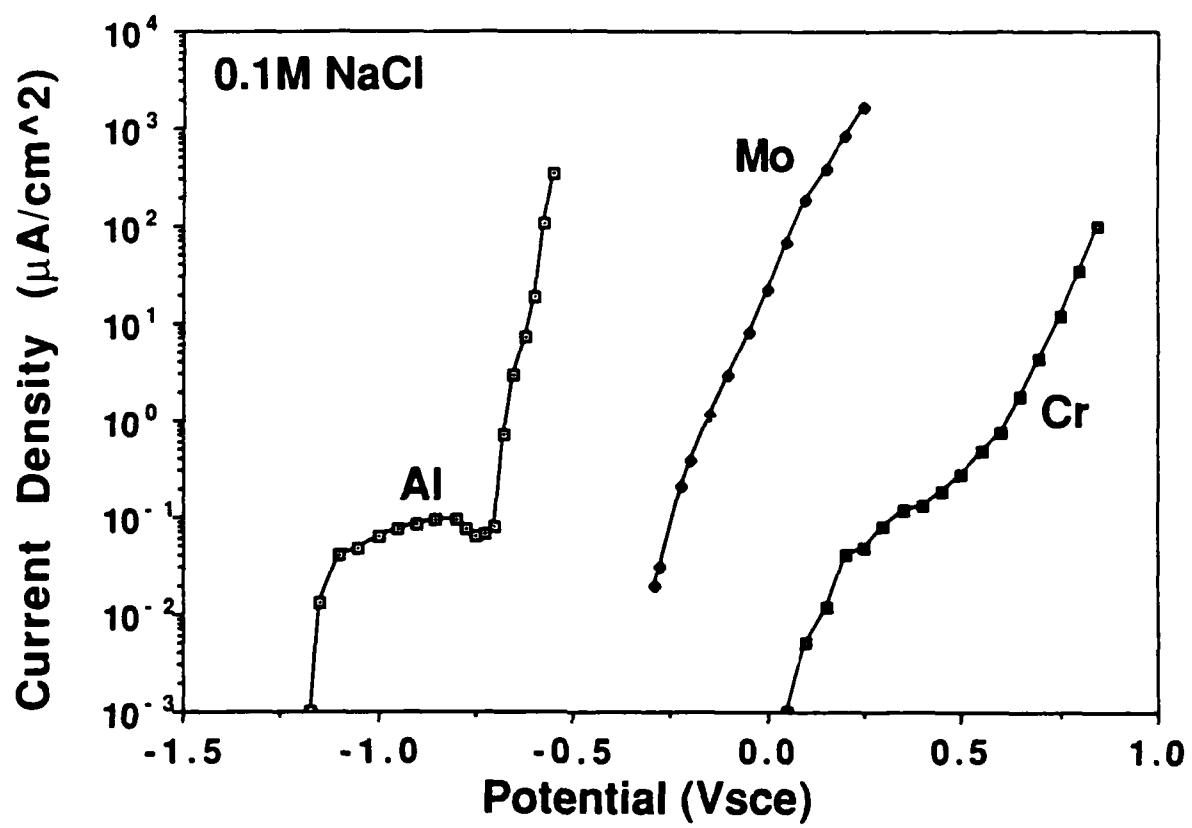


Figure 2. Anodic polarization curves for aluminum, molybdenum, and chromium.

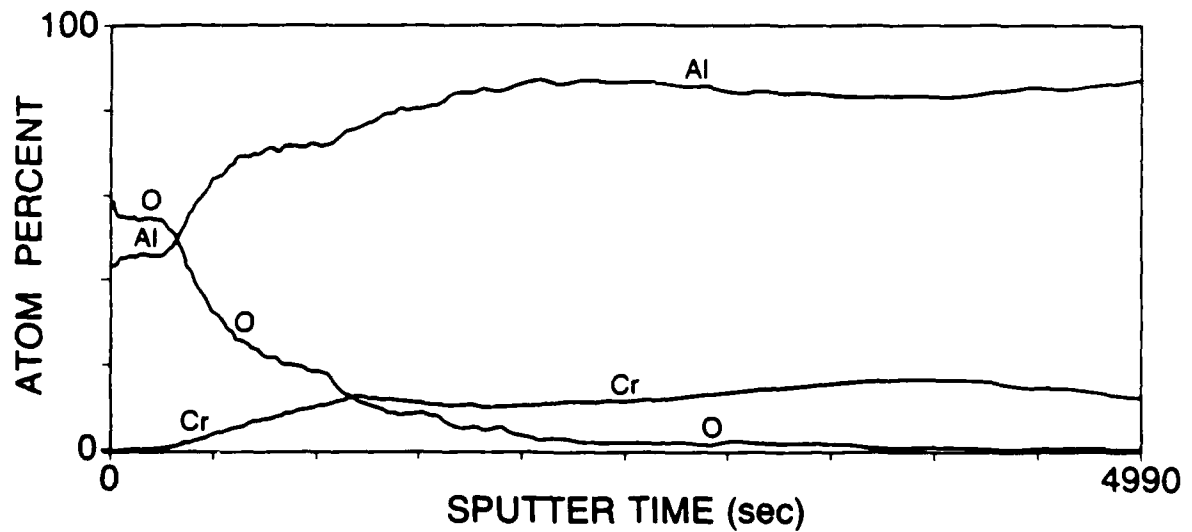


Figure 3. XPS depth concentration profile for a nominal 12 a/o Cr-Al surface alloy.

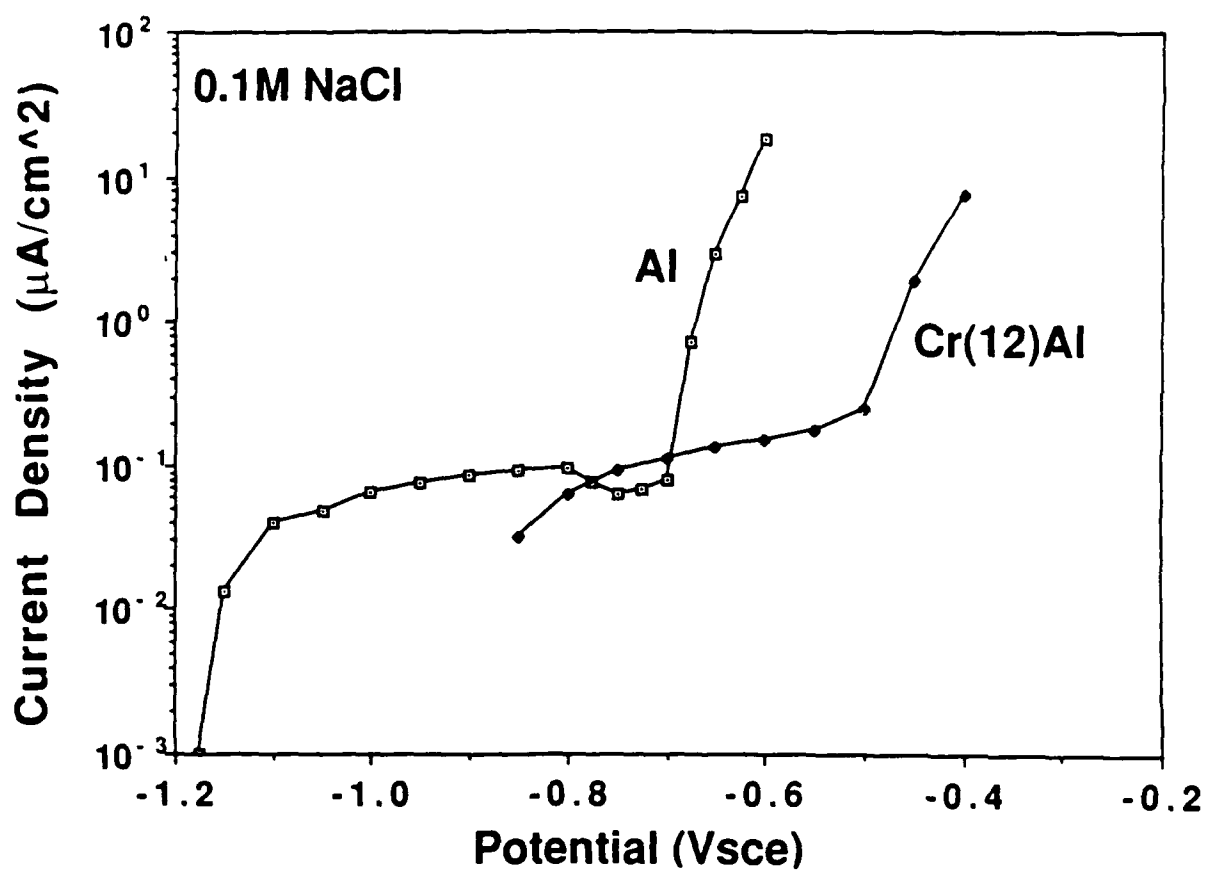


Figure 4. Anodic polarization curves for aluminum and a nominal 12 a/o Cr-Al surface alloy.

Table 1. Ion implantation conditions and pitting potentials in 0.1 M NaCl.

Implanted Ion	Accelerating Voltage (keV)	Dose (x10 <sup>16</sup> ions/cm <sup>2</sup> )	E <sub>pit</sub> (V <sub>SCE</sub> )
None	-	-	-0.700
Mo	25	1	-0.545
	95	2.8	
Cr	25	1.8	-0.585
	95	5.2	
Mo+Cr	25 (Mo)	0.35	-0.565
	95 (Mo)	0.79	
	25 (Cr)	2	
	95 (Cr)	5	

\*Compared to pure aluminum

for implantation with Cr, Mo, and Cr+Mo. The increase in pitting potential varies from 0.115V to 0.155V for the three cases.

As noted above, the  $\text{pH}_{\text{pzc}}$  affects the surface charge and therefore, the adsorption characteristics of an oxide. In neutral solutions the surface of aluminum oxide consists of acidic sites (8,9) which are receptors for Lewis bases such as  $\text{Cl}^-$  whereas  $\text{MoO}_3$ ,  $\text{SiO}_2$ , and  $\text{Cr}_2\text{O}_3$ , for example, are composed of basic sites (8-10) to which  $\text{Cl}^-$  would not be attracted. As shown in Figure 3, the implanted cations are contained in the surface oxide film so that the effect of ion implantation is to replace a portion of the aluminum-oxygen bonds in the passive film with bonds formed between oxygen and the implanted ions. Therefore, ion beam modification offers the possibility of inhibiting  $\text{Cl}^-$  ion adsorption by changing the  $\text{pH}_{\text{pzc}}$  of the surface and thereby, extending the passive range. However, in view of the modest improvement in pitting potentials due to the low concentration of implanted ions in the oxide film, attention was next given to ion beam mixing as the surface modification technique of interest.

### C. Ion Beam Mixing

Figure 5 shows an XPS depth concentration profile for a sample in which a 280 Å film of Mo was vapor deposited onto an Al substrate and subsequently mixed with a 110 keV  $\text{Cr}^+$  ion beam. It can be seen that partial mixing occurred at what had been the Mo/Al interface, but that the outer portion of the coating remained pure Mo. Figure 6 shows anodic polarization curves for Mo, a 270Å Mo film deposited on Al, and a 280Å Mo film deposited on Al and mixed with a 110 keV  $\text{Cr}^+$  ion beam. The polarization curve for the 270Å Mo film deposited on Al shows a small

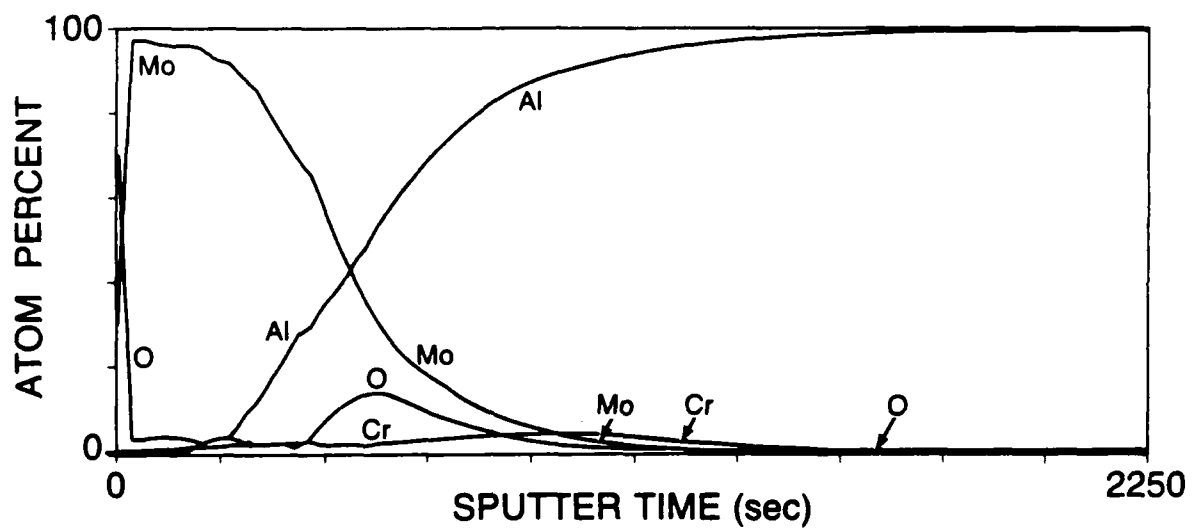


Figure 5. XPS depth concentration profile for a sample in which a 280Å molybdenum coating on aluminum was ion beam mixed with 110 keV Cr<sup>+</sup>.

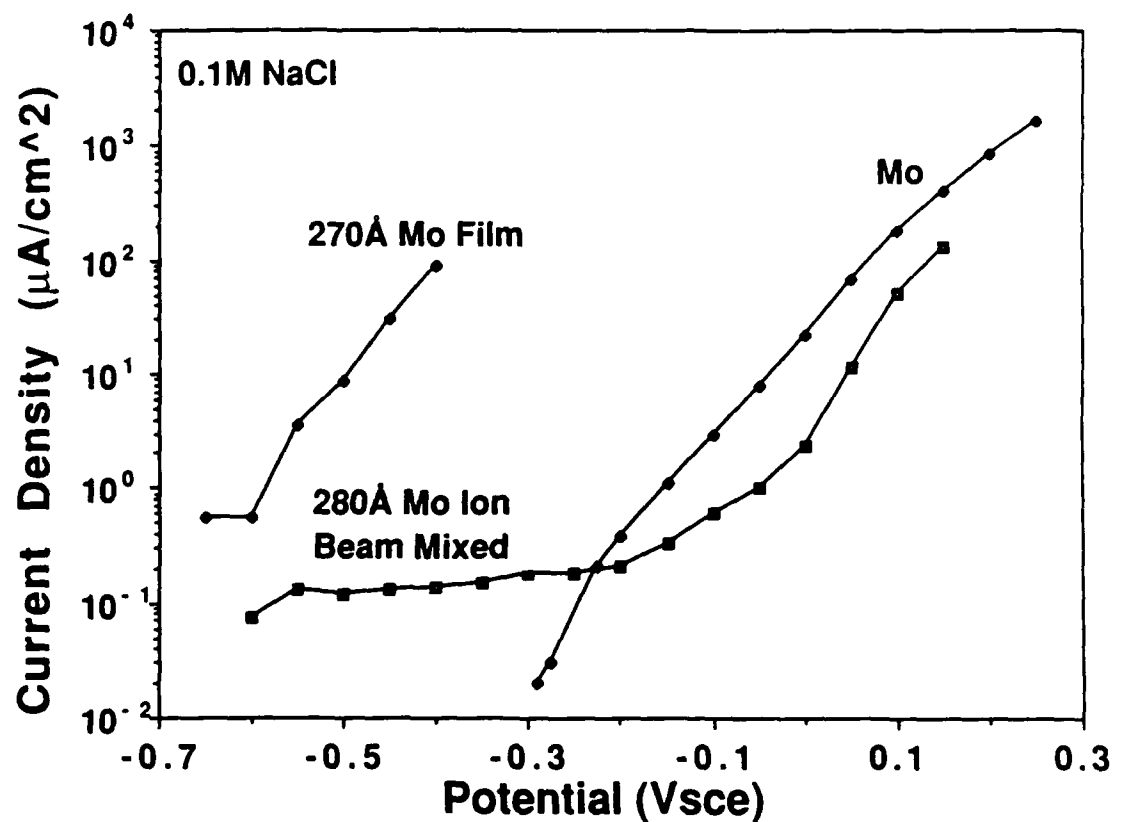


Figure 6. Anodic polarization curves for molybdenum, a  $270\text{\AA}$  molybdenum film deposited on aluminum, and a  $280\text{\AA}$  molybdenum film deposited on aluminum and ion beam mixed with  $110\text{ keV Cr+}$ .

region of stable behavior followed by pitting, whereas the polarization curve for the Mo-Al ion beam mixed sample shows a large region of passivity (400mV) until the polarization curve for the ion beam mixed sample intersects the curve for the Mo sample, i.e. the electrode potential is shifted into the region where molybdenum dissolves. At that and higher potentials the sample behaves similarly to Mo and undergoes general dissolution until at potentials above -0.050 Vsce pitting occurs.

Table 2 summarizes the pitting potential measurements for the ion beam mixed surface alloys. It can be seen that vapor deposition of Mo increases the pitting potential (relative to pure Al) by 50mV, whereas subsequent ion beam mixing provides a total increase of 100 to 650mV. It should be noted that in the better of these two results (mixing with Cr<sup>+</sup>), the improvement is not due to the presence of chromium ions at the surface as chromium is buried beneath the outer surface and does not begin to appear until near the region of mixing. In addition, it should be noted that pitting occurs after the ion beam mixed sample first undergoes general dissolution. That the Mo ion beam mixed sample would undergo general dissolution is not surprising since, as shown in Figure 5, the outer portion of the coating was Mo.

RBS analysis provided additional evidence that general dissolution occurred on the ion beam mixed sample. For example, a comparison of the areas of the Mo RBS peaks before and after polarization (Figure 7) showed that approximately 70% of the Mo was lost during polarization. The remaining Mo was incorporated in the aluminum oxide film that was present on the Al substrate before deposition of the Mo. Figure 8 shows the individual Mo peaks collected for each step of the depth concentration profile presented in Figure 5. At the first step, accumulated before

Table 2. Ion beam mixing conditions and pitting potentials in 0.1M NaCl.

Deposition	Mixing Conditions	Dose ( $\times 10^{16}$ ions/cm $^2$ )	$E_{pit}$ (V <sub>SCE</sub> )	$\Delta E_{pit}^*$ (V)
None	None	-	-0.700	-
Vapor deposition Mo(270Å)	None	-	-0.650	+0.050
Vapor deposition Mo(300Å)	Xe <sup>++</sup> , 250 keV	3.5	-0.600	+0.100
Vapor deposition Mo(280Å)	Cr <sup>+</sup> , 110 keV	3.0	-0.050	+0.650
Sputter deposition Mo(100Å)	None	-	-0.650	+0.050
Sputter deposition Mo(100Å)	Mo <sup>+</sup> , 190 keV	0.5	-0.600	+0.100
Sputter deposition Mo(100Å)	Mo <sup>+</sup> , 190 keV	1.5	-0.600	+0.100
Sputter deposition Cr(100Å)	None	-	-0.600	+0.100
Sputter deposition Cr(100Å)	Cr <sup>+</sup> , 120 keV	1	-0.575	+0.125
Sputter deposition Cr(100Å) +Mo(100Å)	None	-	-0.600	+0.100
Sputter deposition Cr(100Å) +Mo(100Å)	Cr <sup>+</sup> , 120 keV	1	-0.575	+0.125

\*Compared to pure aluminum

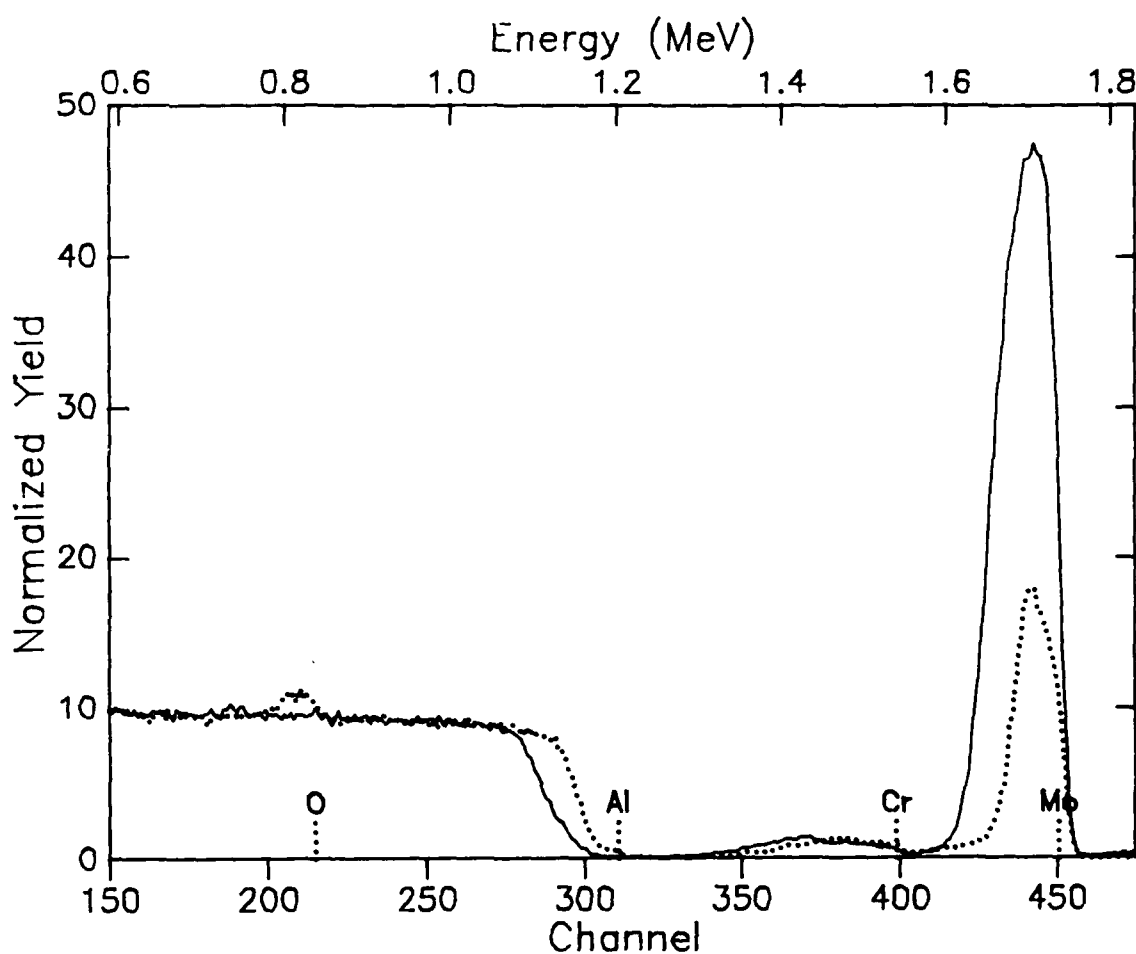


Figure 7. RBS profiles before (solid line) and after polarization (dotted line) of a sample in which a 280 Å molybdenum coating on aluminum was ion beam mixed with 110 keV Cr.

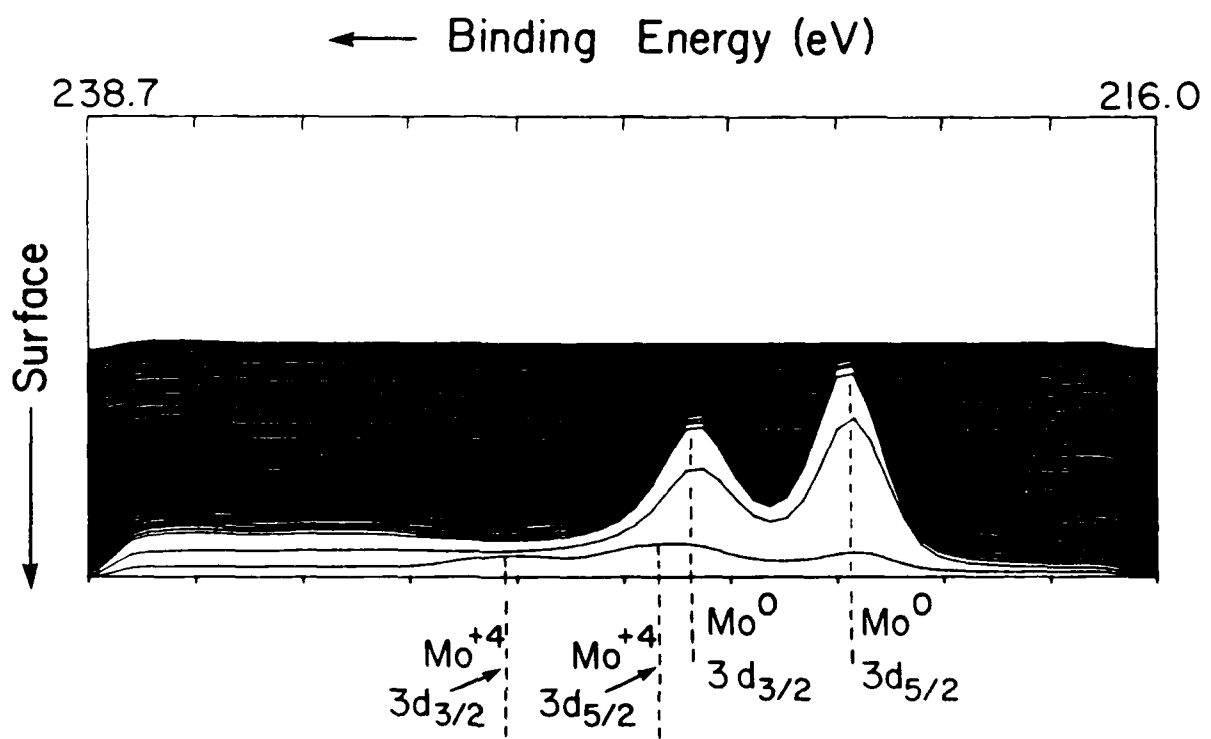


Figure 8. Individual molybdenum XPS peaks collected at each step of the XPS depth concentration profile shown in Figure 5.

sputtering, peaks corresponding to Mo metal and oxidized Mo were observed. A more detailed analysis showed that the oxidized Mo was present as  $\text{Mo}^{+4}$  and  $\text{Mo}^{+6}$ . Subsequent data accumulations, taken after each sputter interval, show only peaks corresponding to Mo metal. Thus the Mo associated with the aluminum oxide film on the Al substrate was present as Mo metal. The increased resistance to pitting of the ion beam mixed sample compared to that of the as-deposited coating presumably occurred because ion beam mixing produced a more compact, less porous coating.

Because there was incomplete mixing with the 270 to 300 $\text{\AA}$  coatings, it was decided to use thinner coatings, i.e. a 100 $\text{\AA}$  Mo coating on Al that was subsequently mixed with a 120 keV  $\text{Mo}^+$  ion beam. The XPS depth concentration profile for the mixed sample was similar to that in Figure 5 but showed that there was a higher degree of mixing compared to samples with the thicker coatings, although the outer surface was still composed of a high percentage of Mo. As in the case of the 280 $\text{\AA}$  film of Mo, the first set of peaks, accumulated before sputtering, show the presence of Mo metal and oxidized Mo, while subsequent peaks show only peaks corresponding to Mo metal. A more detailed analysis showed that the oxidized Mo at the surface was present as  $\text{Mo}^{+4}$  and  $\text{Mo}^{+6}$ . The Al to Mo ratio in the outer portion of this film (approximately the first 30 $\text{\AA}$ ) was 1:4 as determined by XPS analysis. A comparison of the XPS depth profiles before and after polarization showed that the thickness of an as-deposited Mo coating decreased by 35% as a result of polarization, indicating that general dissolution as well as pitting was occurring.

Since the ion beam mixing doses used to produce the samples described above did not provide the desired degree of mixing, the mixing dose was

increased (from 0.5 to  $1.5 \times 10^{16}$  ions/cm<sup>2</sup>). See Table 2 for details. Figure 9 shows a XPS depth concentration profile for a 100Å Mo film mixed at the higher dose. The profile shows a much higher degree of mixing with the Al to Mo ratio being 35:1. An XPS examination of the surface before sputtering showed that about 1 a/o of the Mo at the surface was present in the form of molybdenum oxides. The concentration of molybdenum oxides in the ion beam mixed alloy was comparable to that of the ion implanted samples, and the pitting potentials were similar; see Tables 1 and 2.

Cr-Al ion beam mixed samples were produced under the conditions described in Table 2. The XPS depth concentration profiles for the 100Å Cr ion beam mixed samples were similar to that of the 100Å Mo ion beam mixed samples that were produced under the same conditions, i.e. there was partial mixing of the substrate and the coating. The ratio of Al to Cr at the surface was 1/20. The polarization curves for a 100Å Cr film deposited on Al and for a 100Å Cr film ion beam mixed with a 110 KeV Cr<sup>+</sup> ion beam were similar to each other, and to the polarization curves for the 100Å Mo mixed and unmixed samples that were produced under the same conditions.

Cr-Mo-Al samples were produced using the conditions described in Table 1. The XPS depth concentration profile showed partial mixing at what had been the Cr/Mo and Mo/Al interfaces. The outer portion of the coating was Cr. The polarization behavior for the as-deposited films and for the ion beam mixed samples again were similar to each other, and to the polarization curves for the 100Å Mo mixed and unmixed samples that were produced under the same conditions.

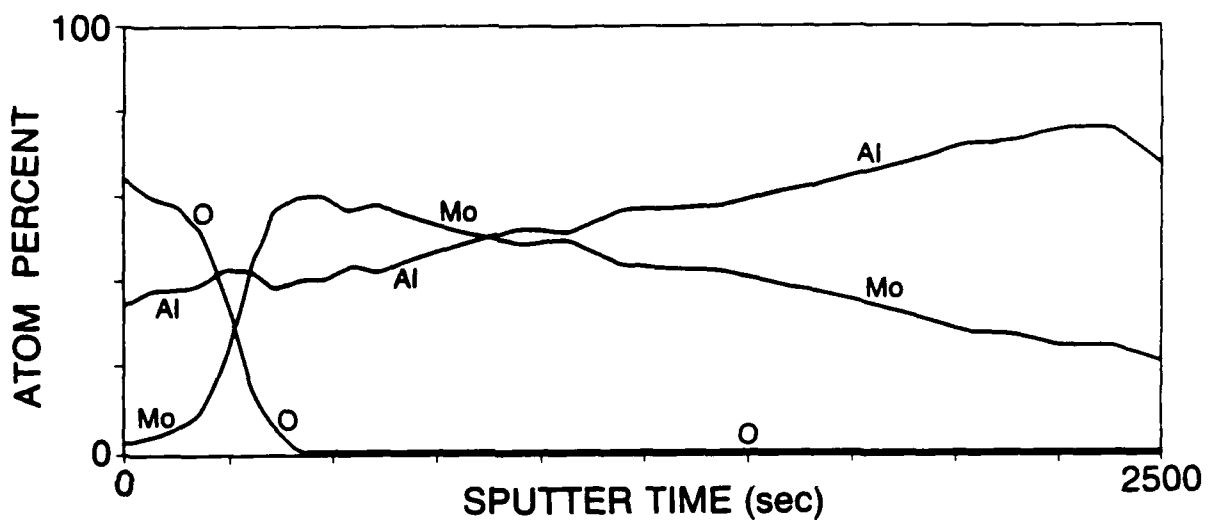


Figure 9. XPS depth concentration profile for a sample in which a 100 $\text{\AA}$  molybdenum coating on aluminum was ion beam mixed with 120 keV Mo $^{+}$ .

In all of the experiments on ion beam mixed samples, the pitting potential was more positive than that for the unmixed coating. However, the increases in pitting potential were generally modest ones (100 to 125mV), with one exception where there was a 650mV increase.

The objective of using ion beam mixing has been to introduce oxide forming elements whose oxides had a pH<sub>pzc</sub> lower than that of Al into the aluminum oxide lattice in concentrations higher than could be accomplished using ion implantation. In the case of ion implantation, the concentration of Mo in the oxide film remained less than 2 a/o even for doses above sputter saturation where the Mo sputter-limited concentration was 20 a/o (2). For ion beam mixing of the 100Å Mo film, two situations were observed: 1) for a dose of  $0.5 \times 10^{16}$  ions/cm<sup>2</sup> Mo, the film was partially mixed at the interface, but remained pure Mo at the surface, and 2) for doses of  $1.5 \times 10^{16}$  ions/cm<sup>2</sup> Mo, the Mo was totally mixed and the Mo concentration in the oxide film was again only 2 a/o. Thus with either ion implantation or ion beam mixing, the ability to control the surface concentration of Mo is complicated by ion induced diffusion/segregation phenomenon. It is known that vacancy defects are mobile at room temperature in Al, so observations of ion induced migration are not surprising. Under the mixing conditions described here, the mixed elements remained almost entirely in the metallic form and the desired mixed oxides were not formed.

Because Al appears in large concentrations at the surface as shown in Figure 9, it is possible to deduce that the mobile species is Al, which migrates from the Mo/Al interface to the surface. Control of the surface concentration of Mo with either ion implantation or ion beam mixing should be possible by performing cold implantations.

#### IV. Summary

Ion implantation was used to produce binary aluminum surface alloys and these alloys had an improved resistance to pitting attack. From the standpoint of the pH<sub>pzc</sub> model this behavior would be explained by the presence of the implanted cations in the stable oxide lattice. There was incomplete mixing of the coating and substrate for the ion beam mixed samples, and the mixed elements remained almost entirely in the metallic state so that the desired mixed oxide films were not formed. The increase in the pitting potentials for the ion beam mixed samples were, in all but one case, similar to the pitting potentials of the ion implanted samples. Mo and Cr did not form stable oxide films in the deaerated 0.1M NaCl and corrosion proceeded by general dissolution.

### V. Acknowledgments

The authors gratefully acknowledge the financial support and technical interaction of A. John Sedriks, Office of Naval Research, Arlington, Virginia. The authors would like to acknowledge and thank W. C. Moshier, Martin Marietta for performing a portion of the XPS analysis. The authors would also like to acknowledge the contributions of Gabrielle T. Peace in sample preparation and electrochemical testing.

## VI. References

1. P. M. Natishan, E. McCafferty, and G. K. Hubler, *J. Electrochem. Soc.*, **135**, 321 (1988).
2. P. M. Natishan, E. McCafferty, and G. K. Hubler, *Mater. Sci. Eng.*, **A116**, 41 (1989).
3. E. McCafferty, P. M. Natishan, and G. K. Hubler, *Corr. Sci.*, **30**, 209 (1990).
4. C. D. Wagner in "Practical Surface Analysis by Auger and X-ray Photoelectron Spectroscopy", p. 478, D. Briggs and M. P. Seah, Eds., John Wiley and Sons, Inc., New York, NY (1983).
5. D. A. Stout, J. B. Lumsden, and R. W. Stahle, *Corrosion*, **35**, 141 (1979).
6. K. Sugimoto and Y. Sawada, *Corr. Sci.*, **17**, 425 (1977).
7. N. D. Greene, C. R. Bishop, and M. Stern, *J. Electrochem. Soc.*, **108**, 836 (1961).
8. W. Stumm and J. J. Morgan, *Aquatic Chemistry*, 2nd. edition, pp. 599-640, Wiley Interscience, New York, NY (1981).
9. G. A. Parks, *Chem. Review*, **65**, 177 (1965).
10. D. E. Yates and T. W. Healy, *J. Colloid Interface Sci.*, **52**, 222 (1975).